



# Increased sedimentation following the Neolithic Revolution in the Southern Levant



Yin Lu<sup>a,b,\*</sup>, Nicolas Waldmann<sup>b</sup>, Dani Nadel<sup>c</sup>, Shmuel Marco<sup>a</sup>

<sup>a</sup> Department of Geophysics, Tel Aviv University, Tel Aviv 6997801, Israel

<sup>b</sup> Dr. Moses Strauss Department of Marine Geosciences, Leon H. Charney School of Marine Sciences, University of Haifa, Mount Carmel 3498838, Israel

<sup>c</sup> The Zinman Institute of Archaeology, University of Haifa, Mount Carmel 3498838, Israel

## ARTICLE INFO

### Keywords:

Dead Sea  
Lacustrine sedimentation  
Surface erosion  
Human impact  
Landscape

## ABSTRACT

The Dead Sea drainage basin offers a rare combination of well-documented substantial climate change, intense tectonics and abundant archaeological evidence for past human activity in the Southern Levant. It serves as a natural laboratory for understanding how sedimentation rates in a deep basin are related to climate change, tectonics, and anthropogenic impacts on the landscape. Here we show how basin-wide erosion rates are recorded by thicknesses of rhythmic detritus laminae and clastic sediment accumulation rates in a long core retrieved by the Dead Sea Deep Drilling Project in the Dead Sea depocenter. During the last ~11.5 kyr the average detrital accumulation rate is ~3–4 times that during the last two glacial cycles (MIS 7c-2), and the average thickness of detritus laminae in the last ~11.6 kyr is ~4.5 times that between ~21.7 and 11.6 ka, implying an increased erosion rate on the surrounding slopes during the Holocene. We estimate that this intensified erosion is incompatible with tectonic and climatic regimes during the corresponding time interval and further propose a close association with the Neolithic Revolution in the Levant (beginning at ~11.5 ka). We thus suggest that human impact on the landscape was the primary driver causing the intensified erosion and that the Dead Sea sedimentary record serves as a reliable recorder of this impact since the Neolithic Revolution.

## 1. Introduction

In addition to tectonics (e.g., Zheng et al., 2000; Dadson et al., 2003; Molnar et al., 2007; Wang et al., 2014) and climatic change (e.g., Molnar, 2001, 2004; Zhang et al., 2001; Clift et al., 2008), humans have also exerted a significant impact on surface erosion over timescales ranging from years to centuries (e.g., Hooke, 2000; Syvitski et al., 2005; Wilkinson, 2005; Montgomery, 2007; Wilkinson and McElroy, 2007; Reusser et al., 2015). However, large-scale anthropogenic impact over millennial timescales remains elusive and unclear. Therefore, there is a need to analyze longer reliable continental records that provide important evidence of the human imprint on landscape evolution. Here, we offer geological evidence for increased sedimentation in the Dead Sea drainage basin, Southern Levant, already at ~11.5 ka. This increase is associated with the establishment of large villages and the concomitant domestication of plants and animals that formed the basis of the Neolithic lifeways. These life styles forever changed the trajectory of human history (Bar-Yosef, 1991; Bar-Yosef, 1998a).

The abundant pre-Neolithic, Neolithic and post-Neolithic archaeological sites in the basin provide unique information on the association

between tectonics, climate change, and increasing human impact on the landscape at the basin-scale. In this study, the clastic sediment accumulation rates (SARs) and the thicknesses of seasonally deposited detritus laminae (Neugebauer et al., 2014, 2015) in a core from the Dead Sea depocenter are used as relative measures of basin erosion. The continuous and well-dated sedimentary record retrieved from the Dead Sea depocenter provides an excellent opportunity for analyzing the response of erosion to climate change, tectonics and anthropogenic activity through time.

## 2. Geological background

The Dead Sea is an endorheic lake bordered by the Jordanian Plateau to the east and the Judean Mountains to the west (Fig. 1A, B). The lake surface is presently ~429 m below sea level. The lake occupies a pull-apart structure (the Dead Sea Basin) that has developed along the Dead Sea Transform since the Miocene (Ben-Avraham et al., 2008). Climatic zones in its drainage basin range from Mediterranean (warm dry summers and mild winters with up to ~1000 mm mean annual precipitation) to hyperarid; these zones fluctuated substantially during

\* Corresponding author at: Department of Geophysics, Tel Aviv University, Tel Aviv 6997801, Israel.  
E-mail addresses: [yinlu@post.tau.ac.il](mailto:yinlu@post.tau.ac.il), [yinlusedimentology@yeah.net](mailto:yinlusedimentology@yeah.net) (Y. Lu).

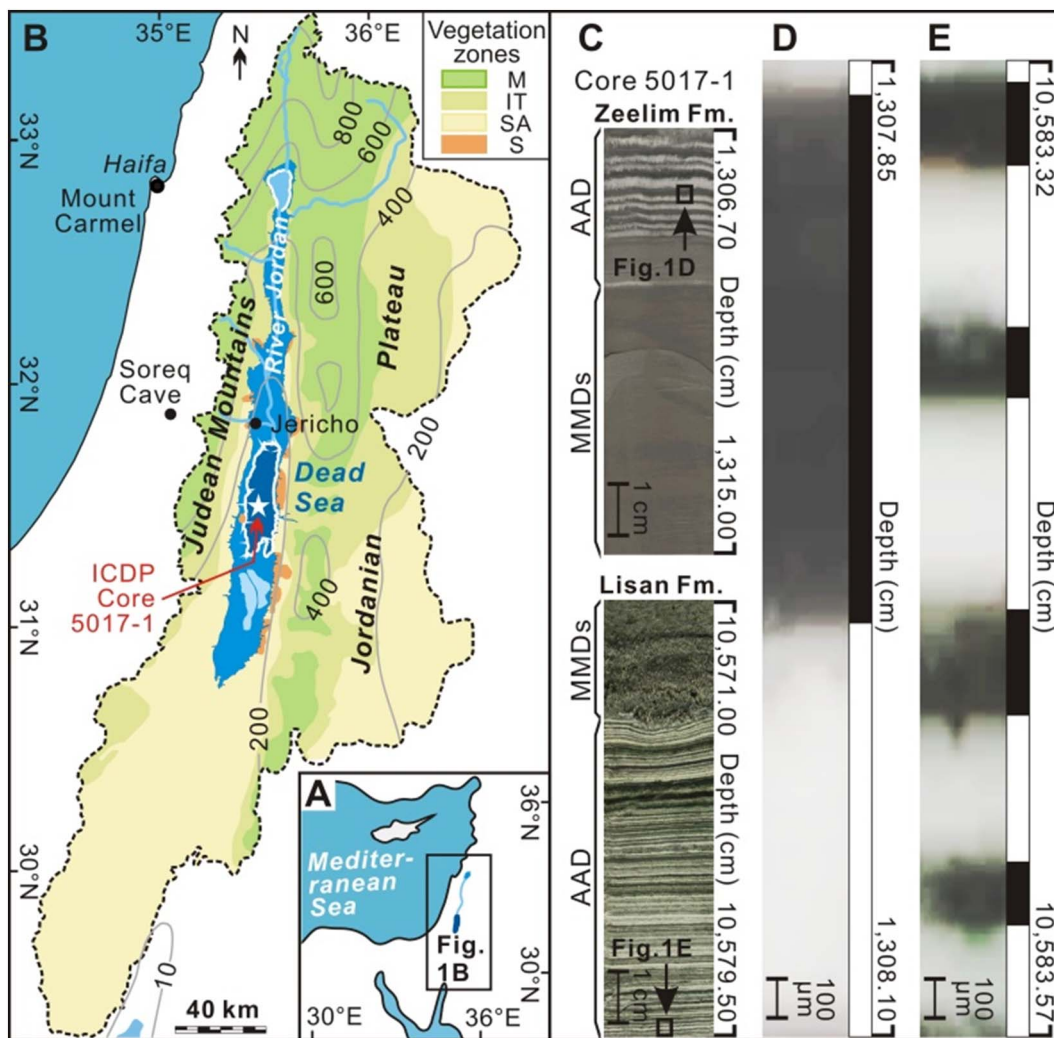


**Fig. 1.** Location and climate of the Dead Sea drainage basin and basic facies of sediments in the Dead Sea depocenter. **A:** Location of the studied area in the Southern Levant. **B:** The Dead Sea drainage basin (enclosed by a black dashed line) with the location of composite core 5017-1 (white star). Current precipitation in  $\text{mm yr}^{-1}$  is marked by gray lines (Enzel et al., 2003) superimposed on vegetation zones (shaded areas) (Langgut et al., 2014) and maximum extent of Lake Lisan (blue area) during the Last Glacial Maximum (LGM) (Bartov et al., 2002). The vegetation zones are divided into M (Mediterranean (humid to semi-humid)), IT (Irano-Turanian (semi-desert)), SA (Saharo-Arabian (desert)), and S (Sudanian (tropical)). Black points mark places referred to this study. **C:** Core images showing alternating laminae of aragonite and detritus (AAD), and mass movement deposits (MMDs) in the formations (Fms.) studied. **D** and **E:** High resolution digital images of the AAD packages showing the thicknesses differences. Black and white bars indicate detritus and aragonite laminae, respectively. (For interpretation of the references to colour in this figure legend, the reader is referred to the web version of this article.)

the Quaternary glacial cycles. During the Quaternary, the basin was consecutively occupied by a sequence of terminal water-bodies: Lake Amora (MIS ~6), Lake Samra (MIS 5), Lake Lisan (MIS 2-4) and the Dead Sea (MIS 1) (Stein, 2001). In accord with these limnological variations, the Quaternary stratigraphy of the basin infill has been divided into four respective formations: Amora, Samra, Lisan, and Zeelim formations.

### 3. Materials, chronology and methods

#### 3.1. Materials

Between November 2010 and March 2011, a ~456.7 m-deep composite core (Core 5017-1) was extracted from ~297.5 m water depth in the Dead Sea depocenter ( $31^{\circ}30'29''\text{N}$ ,  $35^{\circ}28'16''\text{E}$ ) during a drilling campaign under the umbrella of the International Continental Scientific Drilling Program (ICDP) (Stein et al., 2011). The average recovery rate was ~84.5%. The core penetrated the entire Zeelim Fm. (~89.3–0 m), Lisan Fm. (~177.0–89.3 m), Samra Fm. (~328.0–177.0 m) and the upper part of the Amora Fm. (~456.7–328.0 m) (Torfstein et al., 2015).

Lacustrine facies in the core are characterized by sequences of alternating laminae of aragonite and detritus (Fig. 1C) (Neugebauer et al., 2014). In addition, there are thicker layers of detritus (mud, sand and gravel) inferred to be mass movement deposits (Fig. 1C). Thicknesses of aragonite and detritus laminae in the upper ~110 m of the core were carefully measured, and clastic SARs in the upper ~110 m and in the entire core were calculated. As aragonite, gypsum, and halite in Core 5017-1 are chemical precipitates, only the detritus laminae and detrital layers are included in calculations of clastic SARs.

#### 3.2. Chronology

Detailed  $^{14}\text{C}$  and U–Th dating published by the Dead Sea Deep Drilling Project (DSDDP) Scientific Team (a complete list of the scientists is available at [www.icdp-online.org](http://www.icdp-online.org)) show that the core spans the time period from ~220 ka to the present (Neugebauer et al., 2014; Neugebauer et al., 2015; Torfstein et al., 2015) (Fig. 2). The upper ~110 m of the core, were deposited since the Last Glacial Maximum (LGM, ~22 ka). Ages (at 109.1 m and 456.7 m) between dated horizons were calculated by linear interpolation. Age points used for age-depth plot and clastic SAR calculation are listed in Table 1.

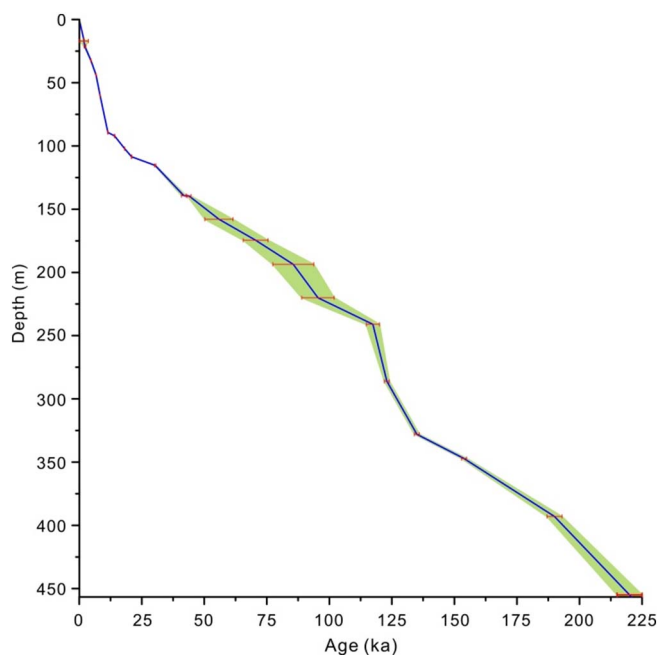


Fig. 2. Age-depth plot of Core 5017-1.  $^{14}\text{C}$  ages with  $1\sigma$  error (Neugebauer et al., 2014; Neugebauer et al., 2015) and U-Th age with  $2\sigma$  error (Torfstein et al., 2015). Age points used for age-depth plot are listed in Table 1.

### 3.3. Methods

#### 3.3.1. Petrography of aragonite-detritus laminae

Representative thin sections from the core were examined with a polarizing microscope.

#### 3.3.2. Measurement of thicknesses of aragonite and detritus laminae

The aragonite and detritus laminae are clearly visible in the core (Fig. 1C) and in high-resolution digital images (Fig. 1D, E). Therefore, no thin sections were used for the thickness measurements. The thicknesses were measured as couplets on high-resolution digital

images with accuracy of 0.1 mm (and estimated to 0.05 mm) using the Corelyzer software. We measured only well-laminated aragonite-detritus couplets and excluded any unclear laminations or severely deformed units.

#### 3.3.3. Clastic SAR calculation

3.3.3.1. Observed clastic SAR. We calculated the observed clastic SAR,  $S$ , as:

$$S(\Delta t) = \frac{D}{\Delta t} \quad (1)$$

where  $D$  is the cumulative thickness of detritus laminae and other clastic layers deposited over time interval  $\Delta t$ .

In the upper  $\sim 110$  m of the core ( $\sim 22$ –0 ka),  $D$  for each time interval,  $\Delta t$ , is determined as:

$$D(\Delta t) = d_{\text{MMDs}} + d_{\text{laminae}} \quad (2)$$

where  $d_{\text{MMDs}}$  is the thickness of mass movement deposits (MMDs; Fig. 1C) and  $d_{\text{laminae}}$  is the cumulative thickness of detritus laminae in the depth interval spanned by  $\Delta t$ . The average clastic SAR during a glacial or interglacial interval (e.g., Holocene, Last Glacial), was calculated as total  $D$  divided by total  $T$ .

In the core from the last glacial period, only a few aragonite and detritus laminae were measured, and in core from the last interglacial, penultimate glacial, and penultimate interglacial (covering MIS 7a–c) periods none were measured. Thus, in calculating the observed clastic SAR for these four pre-postglacial periods ( $\sim 456.7$ –89.3 m,  $\sim 220.8$ –11.5 ka),  $D$  for each glacial or interglacial period is given by:

$$D = L - E - N \quad (3)$$

where  $L$  is the length of core interval during period in question,  $E$  is the thickness of evaporates deposited during that period and  $N$  is the thickness of core intervals with no sediment recovery during the period.

In Eq. (3),  $E$  is given by:

$$E = H + G + A \quad (4)$$

where  $H$ ,  $G$  and  $A$  are the thickness of halite layers, gypsum layers and aragonite laminae, respectively during each period. Here,  $A$  for

Table 1

Age points used for age-depth plot and clastic SAR calculation.

Age (ka)	Core depth (m)	Dating method	Reference
0	0		
1.844 ± 0.026	15.89	$^{14}\text{C}$ cal age (± 1σ)	Neugebauer et al., 2015
1.931 ± 0.025	16.54	$^{14}\text{C}$ cal age (± 1σ)	Neugebauer et al., 2014
1.858 ± 1.839	16.94	U-Th age (± 2σ)	Torfstein et al., 2015
2.266 ± 0.317	21.25	U-Th age (± 2σ)	Torfstein et al., 2015
4.673 ± 0.085	32.36	$^{14}\text{C}$ cal age (± 1σ)	Neugebauer et al., 2015
6.692 ± 0.056	43.75	$^{14}\text{C}$ cal age (± 1σ)	Neugebauer et al., 2014
8.348 ± 0.057	60.11	$^{14}\text{C}$ cal age (± 1σ)	Neugebauer et al., 2014
11.440 ± 0.119	89.25	$^{14}\text{C}$ cal age (± 1σ)	Neugebauer et al., 2014
14.145 ± 0.115	92.06	$^{14}\text{C}$ cal age (± 1σ)	Neugebauer et al., 2014
18.140 ± 0.045	102.10	U-Th age (± 2σ)	Torfstein et al., 2015
20.942 ± 0.131	108.51	$^{14}\text{C}$ cal age (± 1σ)	Neugebauer et al., 2014
30.340 ± 0.261	115.37	$^{14}\text{C}$ cal age (± 1σ)	Neugebauer et al., 2014
41.799 ± 0.935	139.27	U-Th age (± 2σ)	Torfstein et al., 2015
43.946 ± 0.717	139.60	$^{14}\text{C}$ cal age (± 1σ)	Neugebauer et al., 2014
55.864 ± 5.627	157.94	$^{14}\text{C}$ cal age (± 1σ)	Neugebauer et al., 2014
70.513 ± 4.926	174.52	U-Th age (± 2σ)	Torfstein et al., 2015
70.0	177.0 (MIS 5/4)	Integration between U-Th ages and $\delta^{18}\text{O}$ stratigraphy	Torfstein et al., 2015
85.557 ± 8.176	193.58	U-Th age (± 2σ)	Torfstein et al., 2015
95.446 ± 6.481	220.03	U-Th age (± 2σ)	Torfstein et al., 2015
117.401 ± 2.637	241.07	U-Th age (± 2σ)	Torfstein et al., 2015
123.0 ± 1	286.1	Interpolated age	Torfstein et al., 2015
135.0 ± 1	328.0 (MIS 6/5)	Integration between U-Th ages and $\delta^{18}\text{O}$ stratigraphy	Torfstein et al., 2015
153.837 ± 0.981	347.23	U-Th age (± 2σ)	Torfstein et al., 2015
190.0 ± 3	393.0 (MIS 7/6)	Integration between U-Th ages and $\delta^{18}\text{O}$ stratigraphy	Torfstein et al., 2015
220.0 ± 5	455.0	Interpolated age	Torfstein et al., 2015
220.82	456.7	Interpolated age	This study

these four pre-postglacial periods is estimated based on the thicknesses of aragonite and detritus laminae in the upper  $\sim 110$  m of the core and lithological observations of the entire core (for a detailed explanation, please see Appendix A 1).

**3.3.3.2. Corrected clastic SAR.** Because average recovery rate of Core 5017–1 was only  $\sim 84.5\%$ , the observed clastic SAR was corrected for the missing segments during each time period. We assumed that within a core interval spanned by a time period,  $\Delta t$ , the ratio of evaporates to clastics in the missing segments was the same as in the recovered core. This is referred to as the corrected clastic SAR - that is, corrected for missing core.

## 4. Results

### 4.1. Petrography of aragonite-detritus laminae

The sequence of alternating aragonite and detritus laminae is composed of millimeter- to submillimeter-scale couplets, each consisting of a white layer of aragonite and a dark layer of detritus (Figs. 1C–E and 3). The detritus laminae are composed of allogenic quartz, calcite and clay and deposited during a rainy season, while, the aragonite laminae are composed of authigenic aragonite crystals deposited during the following dry season (Prasad et al., 2004; Haliva-Cohen et al., 2012; López-Merino et al., 2016).

### 4.2. Thicknesses of detritus laminae during the last $\sim 22$ kyr

A total of 2500 aragonite-detritus couplets were measured. Thicknesses and distribution of these laminae show two distinct phases, with a transition at  $\sim 89.4$  m ( $\sim 11.6$  ka). From  $\sim 21.7$  to  $11.6$  ka, detritus laminae are thin and densely distributed (Fig. 4A); the average thickness of 1848 detritus laminae is only  $\sim 0.44$  mm (Fig. 4B). Between  $\sim 11.6$  ka and the present, detritus laminae are thicker and sparsely distributed; average thickness of 652 detritus laminae is  $\sim 2.09$  mm (Fig. 4).

### 4.3. Clastic SAR during the last $\sim 22$ kyr

The distribution of clastic SAR is also characterized by two distinct phases, with a transition at  $\sim 89.3$  m ( $\sim 11.5$  ka; Fig. 5B). From  $\sim 21.7$  to  $11.5$  ka, the mean observed and corrected clastic SARs are

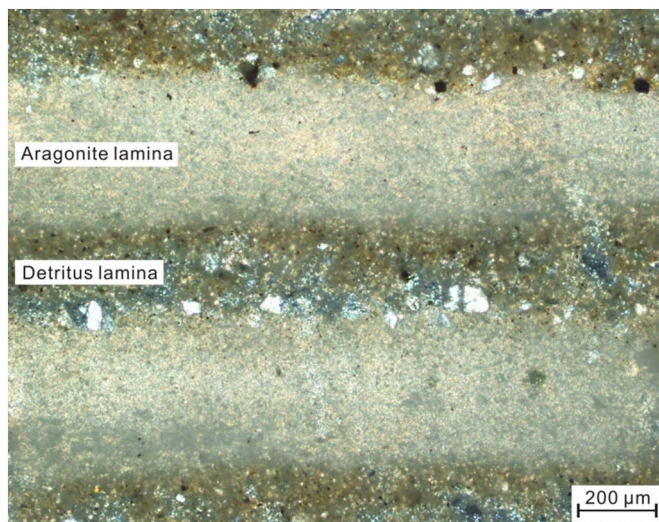


Fig. 3. Photomicrograph of a representative thin section showing aragonite-detritus laminae in Core 5017–1 (core depth:  $\sim 224.45$  m).

$\sim 1.4$  mm yr $^{-1}$  and  $\sim 1.7$  mm yr $^{-1}$ , respectively (ranges:  $\sim 0.6$ – $1.8$  mm yr $^{-1}$  and  $\sim 0.6$ – $2.3$  mm yr $^{-1}$ , respectively) (Fig. 5B). Since  $\sim 11.5$  ka, the means are  $\sim 3.5$  mm yr $^{-1}$  and  $\sim 4.9$  mm yr $^{-1}$ , respectively (ranges:  $\sim 1.5$ – $5.8$  mm yr $^{-1}$  and  $\sim 2.9$ – $7.2$  mm yr $^{-1}$ , respectively) (Fig. 5B and Table 2). The mean corrected clastic SAR since  $\sim 11.5$  ka is  $\sim 3$  times that between  $\sim 21.7$  and  $11.5$  ka.

### 4.4. Clastic SAR of the four pre-postglacial periods ( $\sim 220$ – $11.5$ ka)

The observed and corrected clastic SARs in the Core 5017–1 during the last  $\sim 220$  kyr are shown in Fig. 6 and Table 3. During the period of  $\sim 220$ – $11.5$  ka, the observed and corrected clastic SARs are ranging from  $\sim 0.1$  to  $\sim 3.5$  mm yr $^{-1}$  and  $\sim 0.1$  to  $\sim 3.6$  mm yr $^{-1}$ , respectively. The mean corrected clastic SARs during the four pre-postglacial periods are ranging between  $\sim 1.1$  and  $1.7$  mm yr $^{-1}$ . Thus, the mean corrected clastic SAR during the Holocene (postglacial, P) is  $\sim 3$ – $4$  times that during the last two glacial cycles (Fig. 6C).

Our detail measurements of the core reveal that during the four pre-postglacial periods ( $\sim 220$ – $11.5$  ka,  $\sim 456.7$ – $89.3$  m), mud accounts for

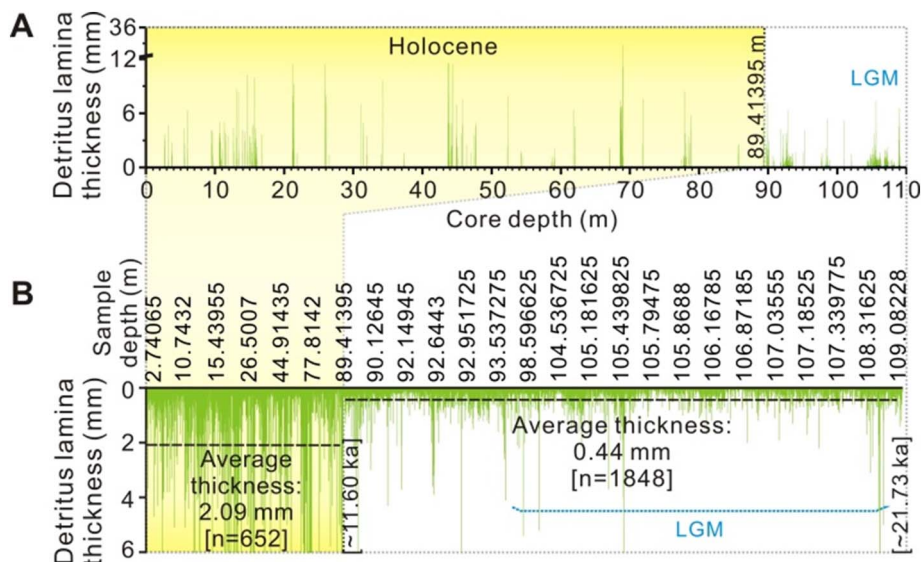
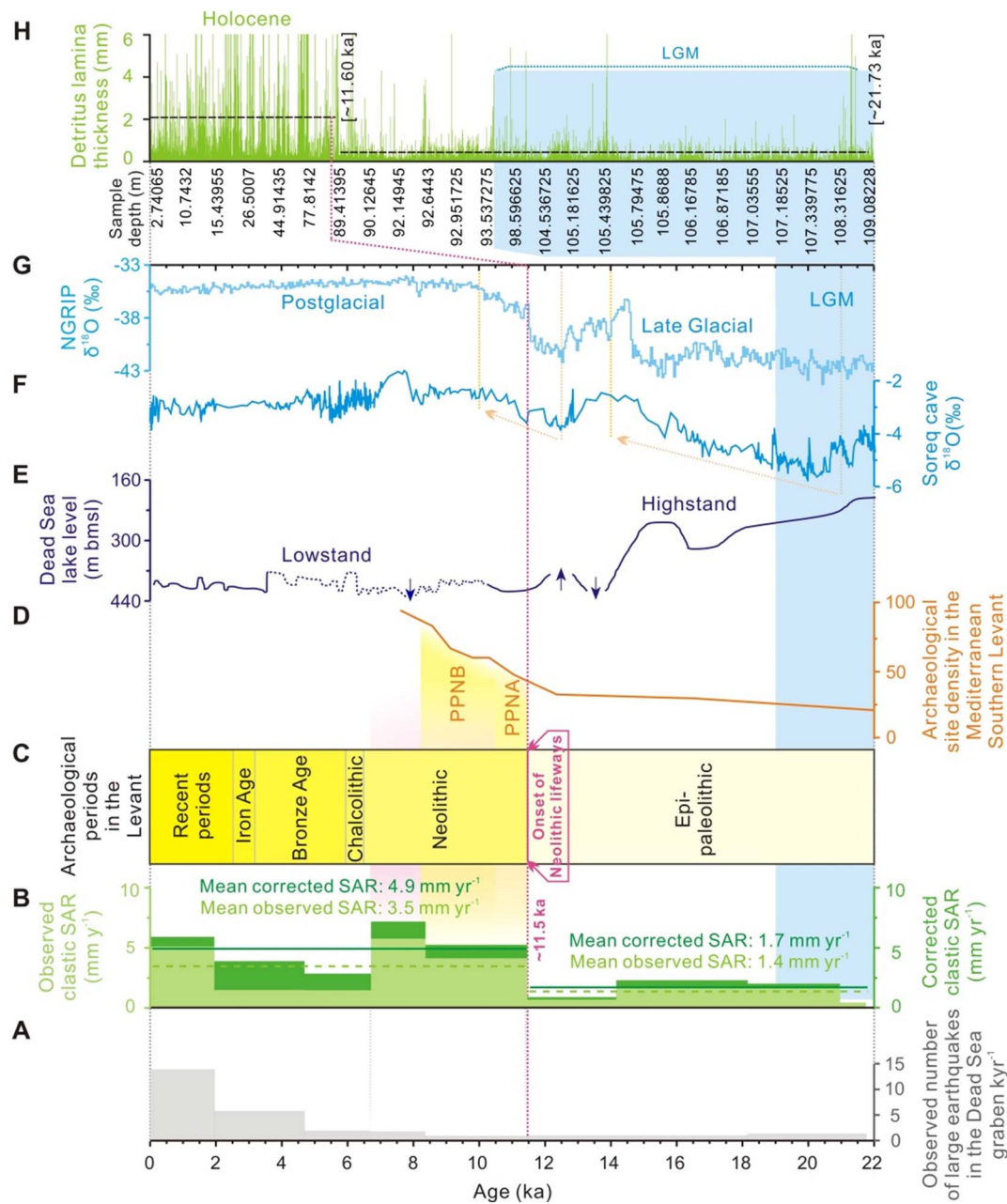


Fig. 4. Distribution and thicknesses of detritus laminae in the upper  $\sim 110$  m of the core ( $\sim 21.7$ – $0$  ka). A: Distribution of detritus laminae in the studied core interval. Detritus laminae are closely-spaced and thin before  $\sim 11.6$  ka ( $\sim 89.4$  m) and more widely spaced and thicker after  $\sim 11.6$  ka. B: In this panel every lamina is plotted sequentially (with its real depth); n, number. Laminae are thicker in the upper  $89.4$  m of the core (since  $\sim 11.6$  ka) but there are more of them per meter between  $89.4$  and  $109.1$  m ( $\sim 21.7$  and  $11.6$  ka).



**Fig. 5.** Correlation of the Dead Sea clastic sediment accumulation rate (SAR) record with global and regional climate proxies, human evolution in the Levant, and tectonic activity in the Dead Sea. A: Observed number of large earthquakes (with local intensity  $\geq V$ ) in the Dead Sea graben per kyr during the last  $\sim 22$  kyr (for a detail information of paleoearthquakes, please refer to Appendix A 2). B: Clastic SAR in the Dead Sea depocenter, based on Core 5017-1. The dashed light green lines represent mean observed clastic SAR and the solid light green lines are mean corrected clastic SAR. C: Archaeological periods in the Levant (Savage and Levy, 2016) (for a detail list, please see Appendix C Table C1). D: Estimates of archaeological site density per kyr in the Mediterranean climate zone of the Southern Levant (Goring-Morris et al., 2009) (Appendix B Fig. B1). PPNA, Pre-Pottery Neolithic A; PPNB, Pre-Pottery Neolithic B. E: Dead Sea lake level (Torfstein et al., 2013); bmsl: below mean sea level. F:  $\delta^{18}O_{\text{speleo}}$  record from Soreq Cave (Fig. 1B) (Grant et al., 2012). The two dashed arrows indicate two periods ( $\sim 21.0$ – $14.0$  ka, and  $\sim 12.5$ – $10.0$  ka) of aridification in the Southern Levant. G: Greenland (NGRIP) (Andersen et al., 2004) ice core  $\delta^{18}O$ . H: Thickness of detritus lamina in the upper  $\sim 110$  m of the Core 5017-1 ( $\sim 21.7$ – $0$  ka). (For interpretation of the references to colour in this figure legend, the reader is referred to the web version of this article.)

$\sim 90\%$  of the total thickness of clastic sediments, while sand and gravel for only  $\sim 10\%$ . The mud has much lower porosity than the sand and gravel. Thus, even if compaction of clastic sediments deposited during the four pre-postglacial periods is as much as  $\sim 10\%$ , the corrected clastic SARs (ranged between  $\sim 1.2$  and  $1.9 \text{ mm yr}^{-1}$ ) are still only  $\sim 1/4$  to  $1/3$  of those during the last  $\sim 11.5$  kyr.

## 5. Discussion

### 5.1. Intensified basin erosion since $\sim 11.5$ ka

Detritus laminae are deposited during rainy seasons (winter)

(Prasad et al., 2004; Haliva-Cohen et al., 2012; López-Merino et al., 2016). Thus, these seasonally deposited laminae are inferred to be a result of basin erosion, and their thicknesses reflect the intensity of erosion in the drainage basin. The average thickness of detritus laminae in the last  $\sim 11.6$  kyr is  $\sim 4.5$  times that during the late glacial,  $\sim 21.7$ – $11.6$  ka (Fig. 4B). This pattern is consistent with previous results obtained from a short core from the Dead Sea margin and a nearby stratigraphic section in an outcrop: between  $\sim 3.3$  and  $1.0$  ka, the average thickness of detritus laminae in the core is  $\sim 1.0$  mm (Migowski, 2001; Neugebauer et al., 2015), and that between  $\sim 26.2$  and  $17.7$  ka in the outcrop is  $\sim 0.3$  mm (Prasad et al., 2004). This pattern indicates the intensified basin erosion since  $\sim 11.6$  ka.

**Table 2**  
Observed and corrected clastic SAR in the Core 5017–1 during the last ~220 kyr.

Age interval (ka)	Core interval (m)	D (m)	Observed S (mm yr <sup>-1</sup> )	Core recovery rate (%)	Corrected S (mm yr <sup>-1</sup> )	Glacial cycle
0–1.931	0–16.54	10.33	5.3	90.5	5.9	P (MIS 1)
1.931–4.673	16.54–32.36	4.10	1.5	38.3	3.9	
4.673–6.692	32.36–43.75	2.97	1.5	54.1	2.9	
6.692–8.348	43.75–60.11	9.54	5.8	80.2	7.2	
8.348–11.440	60.11–89.25	12.77	4.1	78.5	5.3	
11.440–14.145	89.25–92.06	1.87	0.7	76.5	0.9	LG (MIS 4-2)
14.145–18.140	92.06–102.10	7.13	1.8	77.4	2.3	
18.140–20.942	102.10–108.51	4.73	1.7	83.5	2.0	
20.942–30.340	108.51–115.37	5.73	0.6	98.2	0.6	
30.340–41.799	115.37–139.27	19.18	1.7	98.6	1.7	
41.799–43.946	139.27–139.60	0.29	0.1	98.5	0.1	
43.946–55.864	139.60–157.94	16.62	1.4	98.4	1.4	
55.864–70.0	157.94–177.00	16.72	1.2	97.7	1.2	
70.0–85.557	177.00–193.58	14.12	0.9	97.9	0.9	LIG (MIS 5)
85.557–95.446	193.58–220.03	15.51	1.6	79.4	2.0	
95.446–117.401	220.03–241.07	13.03	0.6	83.4	0.7	
117.401–123.0	241.07–286.01	19.35	3.5	95.3	3.6	
123.0–135.0	286.01–328.00	28.88	2.4	84.5	2.8	
135.0–153.837	328.00–347.23	14.67	0.8	87.9	0.9	PG (MIS 6)
153.837–190.0	347.23–393.00	34.66	1.0	83.7	1.1	
190.0–220.0	393.00–455.00	42.29	1.4	81.5	1.7	PIG (MIS 7c-a)
220.0–220.82	455.00–456.69	1.36	1.7	84.6	2.0	

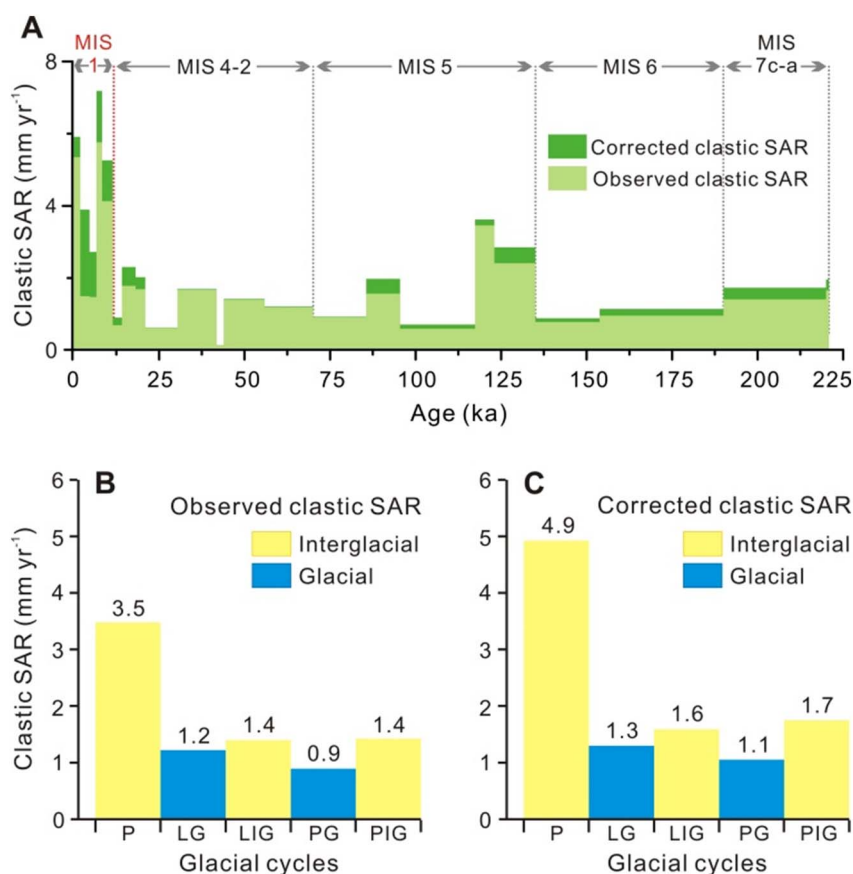


**Fig. 6.** Comparison of clastic SAR between postglacial (~11.5–0 ka) and pre-postglacial periods. A: Clastic SAR in the Core 5017–1 during the last ~220 kyr. B: Observed clastic SAR during the five glacial-interglacial periods. C: Corrected clastic SAR during the five glacial-interglacial periods (corrected for missing core sections; Tables 2 and 3). P, postglacial (MIS1; ~11.5–0 ka); LG, last glacial (MIS4-2; ~70–11.5 ka); LIG, last interglacial (MIS5; ~135–70 ka); PG, penultimate glacial (MIS6; ~190–135 ka); PIG, penultimate interglacial (MIS 7c-a; ~220.8–190 ka).

Modern sedimentation monitoring at the Dead Sea depocenter yields a detritus flux of ~3.2–6.4 mm yr<sup>-1</sup> (Stiller et al., 1997) (Appendix A 3). This is consistent with our mean corrected clastic SAR of ~4.9 mm yr<sup>-1</sup> since ~11.5 ka. Clastics reaching the Dead Sea depocenter are mainly intrabasinal alluvial sediments and external eolian dust (Haliva-Cohen et al., 2012). Modern measurements of dust

deposition yield an average SAR of < 0.04 mm yr<sup>-1</sup> (Singer et al., 2003); we take this as an average for the postglacial period (Appendix A 4). This is negligible compare with our estimate of ~4.9 mm yr<sup>-1</sup> of clastic deposition during this period. Thus the increase in average clastic SAR since ~11.5 ka, implies an increased erosion rate (e.g., Zhang et al., 2001; Clift, 2006) in the basin.

**Table 3**  
Observed and estimated clastic SAR for the Holocene and last two glacial cycles (MIS 7c-2).

Glacial cycle	Age period (ka)	Core interval (m)	T (ka)	D (m)	H + G (m)	A (m)	Mean observed S (mm yr <sup>-1</sup> )	Core recovery rate (%)	Mean corrected S (mm yr <sup>-1</sup> )
P (MIS 1)	0–11.5	0–89.3	11.5	39.7	23.3	0.8	3.5	70.5	4.9
LG (MIS 4-2)	11.5–70.0	89.3–177.0	58.6	71.6	1.5	9.2	1.2	94.1	1.3
LIG (MIS 5)	70.0–135.0	177.0–328.0	65.0	90.9	36.3	5.9	1.4	88.1	1.6
PG (MIS 6)	135.0–190.0	328.0–393.0	55.0	49.2	1.3	4.6	0.9	85.0	1.1
PIG (MIS 7c-a)	190.0–220.8	393.0–456.7	30.8	43.8	7.1	1.2	1.4	81.6	1.7

## 5.2. Climatic and tectonic-driven erosion during the four pre-postglacial periods (~220–11.5 ka)

In the Levant, as in other parts of the old world, the environmental impact of Pleistocene hominins was minimal, as they were organized in small nomadic bands, hunting and gathering only on the scale needed by each group (Foley et al., 2013). Basin erosion was thus driven primarily by climate and tectonic events during this time period (~220–11.5 ka). The climatic regime of the basin is generally arid with lower lake stands during interglacials (Fig. 5 E–G) in comparison with glacial periods (Bar-Matthews et al., 2003; Waldmann et al., 2010; Grant et al., 2012; Torfstein et al., 2013), although there were some climatic fluctuations during both interglacial and glacial periods (Bar-Matthews et al., 2003; Grant et al., 2012). The sinistral slip rate on the Dead Sea fault has been stable at ~5 mm yr<sup>-1</sup> during the Pleistocene and Holocene (Marco and Klinger, 2014). Thus, the general periodic climate regime and stable episodic slip on the fault are likely to have resulted in only minor fluctuations and cannot account for the two to three fold increase in clastic sedimentation rate in the last ~11.5 kyr (Fig. 6C).

It is widely accepted that there is a time lag of tens of thousands to millions of years in landscape response to climate change; thus steady-state topography and steady-state denudation are unlikely to be attained during the Quaternary climate oscillations (Whipple, 2001; Zhang et al., 2001). However, various studies have documented that vegetation is sensitive to climate change, and the time lag is short (Allen and Breshears, 1998; Breshears et al., 2005; Kelly and Goulden, 2008; Litt et al., 2012). In the Southern Levant, precipitation is the primary factor limiting vegetation (Miebach et al., 2015). A reduction in vegetative cover during the relatively arid interglacial periods would have led to an increase in erosion of shallow mountain soils (Allen and Breshears, 1998; Montgomery et al., 2000; Istanbuloglu, 2005; Vanacker et al., 2007). Consequently, clastic SARs during the two late Pleistocene interglacial periods are slightly higher than during the subsequent glacial periods (Fig. 6).

These relatively minor fluctuations in detritus flux (~1.1–1.7 mm yr<sup>-1</sup>) during the late Pleistocene, implying relatively gradual and minor fluctuations in basin erosion primarily driven by climate and tectonic activities, can be taken as the background level for comparison with the intensified erosion during the Holocene. The detrital flux during the last two glacial cycles is ~1/4 to 1/3 that during the Holocene, suggesting that other driver(s), most likely, anthropogenic, should be sought to explain the increased sedimentation.

## 5.3. Tectonic and climatic regimes of the basin during the last ~22 kyr

### 5.3.1. Tectonic factor

Tectonic uplift that steepens slopes or large earthquakes that trigger landslides, mobilizing large volumes of clastic sediments, can lead to abrupt increases in sediment flux in a very short time (Parker et al., 2011; Marc et al., 2015; McHugh et al., 2016). Uplift of the Dead Sea margin has been significant during the late Pleistocene but negligible during the Holocene (Bartov et al., 2006). As this is the reverse of the sedimentation rate pattern, uplift does not appear to have

been a factor in the Holocene increase in sedimentation rate.

There were also relatively few large paleoseismic events (with local intensity ≥ V) along the Dead Sea margin in the late Pleistocene and early Holocene (between ~21.7 and 4.7 ka) (Fig. 5A; Appendix A 2) (Marco et al., 1996; Ken-Tor et al., 2001; Migowski et al., 2004; Agnon et al., 2006). Such events, those with an intensity ≥ V in the Dead Sea drainage, although possibly occurring some distance away, should have played a role in basin erosion and sedimentation. As the sedimentation rate increased by a factor of 2 during the period of seismic quiescence between ~11.5 and 4.7 ka (Fig. 5A, B), it also appears that earthquakes are unlikely to have acted as a primary driver of the intensified erosion after ~11.5 ka.

### 5.3.2. Climatic factor

Aridification may either decrease sediment yields due to the decrease in rainfall (Lague et al., 2005; Molnar et al., 2006) or increase yields due to the increase in relative magnitudes of rare floods (Molnar, 2001; Molnar et al., 2006) and the reduction in vegetative cover (Allen and Breshears, 1998; Montgomery et al., 2000; Istanbuloglu, 2005; Vanacker et al., 2007). During the last deglaciation, there were two periods of aridification in the Southern Levant, one between ~21.0 and 14.0 ka, another between ~12.5 and 10.0 ka (Fig. 5F). During the first of these, the corrected clastic SAR in the Dead Sea depocenter was ~2.2 mm yr<sup>-1</sup> (Fig. 5B), the highest rate during the last glacial period. However, 2.2 mm yr<sup>-1</sup> is still less than half that during the last ~11.5 kyr (~4.9 mm yr<sup>-1</sup>). This implies that aridification between ~12.5 and 10.0 ka is unlikely to account for the increase in sediment flux from ~0.9 mm yr<sup>-1</sup> to ~5.3 mm yr<sup>-1</sup> and then 7.2 mm yr<sup>-1</sup> in the early Holocene (Table 2).

The Dead Sea lake level drop between the LGM and ~14.0 ka (Fig. 5E) exposed large expanses of previously submerged areas to erosion and shortened the distance between the drill site and the lakeshore. However, the drill core does not show a significant increase in clastic SAR (Fig. 5B) or in thickness of detritus laminae (Fig. 4B) during the lake level drop, or shortly after it (~14.0–11.5 ka). Thus, neither the lake level drop nor the shoreline proximity can account for the increased sedimentation.

However, the increase in sediment flux at ~11.5 ka, correlates closely with the establishment of Neolithic lifeways in the Southern Levant (Fig. 5C, D), suggesting that, most likely, the anthropogenic factor was the primary driver of the intensified erosion since ~11.5 ka.

## 5.4. Anthropogenic factor as primary driver of the increased Holocene sedimentation

### 5.4.1. Impact of establishing permanent large villages

In the Levant, it has been only since the Neolithic Revolution (beginning at ~11.5 ka) that human communities completely changed their previous way of life (Bar-Yosef, 1998a), settling down in large villages, developing agriculture based on domesticated cereals, legumes, sheep and goats, and creating a new momentum, with ever-increasing impact on the landscape at the basin scale. The Levant is the first place where this change in lifestyle occurs (Bar-Yosef, 1998a). During the Pre-Pottery Neolithic A (PPNA; ~11.5–10.5 ka), large villages were established in various ecological niches within the basin

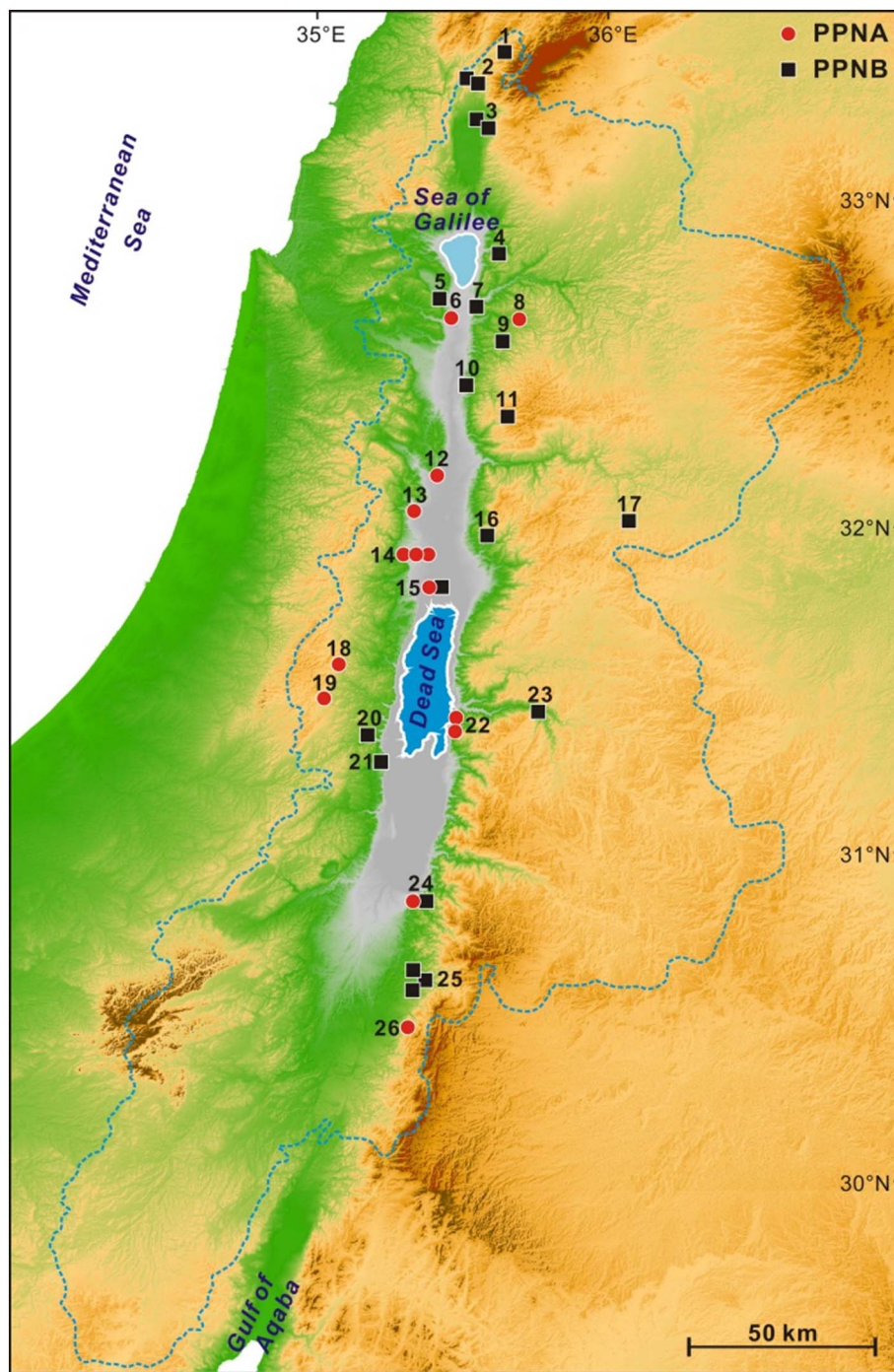


Fig. 7. Distribution of large villages within the Dead Sea drainage basin during the PPNA (~11.5–10.5 ka) and PPNB (~10.5–8.2 ka) (Kenyon, 1957; Lechevallier, 1978; Noy, 1989; Rollefson and Köhler-Rollefson, 1989; Bar-Yosef, 1991; Byrd, 1994; Bar-Yosef and Gopher, 1997; Rollefson, 1997; Kuijt and Goring-Morris, 2002; Edwards and House, 2007; Goring-Morris et al., 2009; Nadel and Nadler-Uziel, 2011). Sites in the map: 1. Hagoshrim; 2. Kfar Giladi, Tel Roim West; 3. Beisamoun, Tel Teo; 4. Mujahiya; 5. Munhata; 6. Gesher; 7. Sha'ar Hagolan; 8. Iraq ed-Dubb; 9. Tell Rakan; 10. Wadi el Yabis; 11. er-Rahib; 12. Huzuk Musa; 13. Ain Suhun; 14. Gilgal, Netiv Hagdud, Salibiya IX; 15. Jericho; 16. Wadi Shu'eib; 17. Ain Ghazal; 18. El-Khiam; 19. Ain Darat; 20. Nahal Hemar; 21. Mezaad Mazal; 22. Dhra, ZAD 2; 23. Es-Sifia; 24. Wadi Fidan 16, Ghweir 1; 25. Beidha, Baja, Shaqarat Msaied; and 26. Sabra 1.

(Bar-Yosef, 1991; Kuijt and Goring-Morris, 2002) (Figs. 5D and 7). Jericho (Figs. 1B and 7), the largest settlement near the Dead Sea, covered ~4 ha and had a population of many hundreds or more (Kenyon, 1957) (Appendix B Fig. B1).

As construction materials for dwellings and public buildings included stone, timber and other perishable materials, the Neolithic villagers would have increasingly depleted their immediate environments of trees, shrubs, and grasses. During the Pre-Pottery Neolithic B (PPNB, ~10.5–8.2 ka), villages expanded (Fig. 5D), and architecture became increasingly massive. Many buildings had two stories, thus

requiring even more construction material. Furthermore, the use of plaster on floors and walls became common (Kenyon, 1957; Lechevallier, 1978), the production of which involved the burning of large quantities of wood. Experiments (Goren and Goring-Morris, 2008) and simulations (Rollefson and Köhler-Rollefson, 1989) indicate that areas up to several kilometers in diameter around villages became treeless within a few generations. Indeed, it is during the end of the PPNB (~8.4–8.2 ka) and immediately thereafter (~8.2–6.7 ka), that the clastic SAR reaches its highest level in the entire core (Fig. 5B, D).

#### 5.4.2. Impact of fauna and flora domestication on landscape

The incorporation of herds of sheep and goats in the economies of farming communities spread rapidly. In many bone assemblages from PPNB villages, the sheep and goat components reach over 50% of all mammals (Davis, 1991; Bar-Yosef, 1998b; Zeder, 2011). Fodder harvesting for these herds, as well as for cattle and pigs which were domesticated by the end of this period, and grazing around the sites must have been intensive. In this relatively dry landscape, constant grazing pressure and intensive fodder harvesting, would have continuously depleted and reduced the natural plant and tree communities and disturbed the soil, making it more erodible. Pastoral groups that thrived in the semi-arid and arid hinterlands with their herds may have also depleted additional areas of trees and shrubs.

Hence, from the onset of the Neolithic settlement pattern and economy, but certainly by the end of the PPNB, the impact on the landscape would have been significant (Perevolotsky and Seligman, 1998). Since then, as in other Old World areas, the influence of human communities on the landscape has continued to increase. As the Southern Levant has been continuously and intensively inhabited since the beginning of the Neolithic, the local natural Mediterranean forests, open park forests and maquis never returned to their original state.

Experimental and modeling studies suggest that vegetation cover reduces erosion at the catchment scale (Istanbulluoglu, 2005; Vanacker et al., 2007). Disturbing vegetation by clearing (either by logging or wildfire) impacts the stabilizing effect of roots on soil, which consequently reduces slope stability and accelerates erosion (Montgomery et al., 2000; Istanbulluoglu, 2005; Portenga et al., 2016). Measurements of sediment flux caused by the 1989 wildfire in Mount Carmel (Fig. 1B), for example, confirm this accelerated erosion (Inbar et al., 1998). Moreover, grazing animals intensify destruction of microscopic biogenic crusts which also enhances erosion (Warren, 2001). Thus, the destruction of vegetation cover leads to increased denudation.

It is widely documented that there is a direct link between human impacts and sediment flux. Sediment flux responds rapidly to anthropogenic impact, not only world-wide (Hooke, 2000; Montgomery et al., 2000; Syvitski et al., 2005; Wilkinson, 2005; Montgomery, 2007; Wilkinson and McElroy, 2007; Hoffmann et al., 2010) but also in the Southern Levant (Ackermann et al., 2005; Avni et al., 2006). As much of the vegetation in the Dead Sea drainage basin was disturbed by humans at the catchment scale following the Neolithic Revolution, land surface erodibility may have increased considerably. We surmise that the 2- to 3-fold increase in sediment flux compared with the period prior to ~11.5 ka is due to this massive human intervention.

## 6. Conclusions

Records of the thicknesses of detritus laminae and clastic SARs from the Dead Sea depocenter indicate intensified basin erosion since ~11.5 ka. The intensified erosion cannot be explained by the tectonic and climatic regimes of the basin. However, the beginning of the period of intensified erosion overlaps with the onset of Neolithic lifeways in the southern Levant. We suggest that drastic depletion of vegetation during the establishment of permanent large villages and the domestication of plants and animals is responsible for a 2 to 3-fold increase in basin erosion rate recorded in the Dead Sea sediments penetrated by Core 5017–1. Thus, humans appear to have been a dominant force shaping the landscape in the Southern Levant for millennia, a much longer time than previously thought.

## Acknowledgments

We thank the funding agencies for this project: the International Continental Scientific Drilling Program (ICDP, 5017) and Israel Science Foundation (ISF; Center of Excellence Grant: #1436/14 to S.M.). We thank Nimer Taha and Ovie Emmanuel Eruteya for help with lab work, Achim Brauer, Daniel Ariztegui, Danny Rosenberg and Or M. Bialik for

their comments, and Ezra S. Marcus for English polish. Special thanks to Prof. Roger LeB. Hooke (University of Maine) for thorough English editing and critical comments that significantly improved the manuscript. Two anonymous reviewers are thanked for providing helpful and constructive comments.

## Appendix A. Supplementary data

Supplementary data to this article can be found online at <http://dx.doi.org/10.1016/j.gloplacha.2017.04.003>.

## References

- Ackermann, O., Bruins, H.J., Maeir, A.M., 2005. A unique human-made trench at Tell es-Sâfi/Gath, Israel: anthropogenic impact and landscape response. *Geochronology* 20, 303–327.
- Agnon, A., Migowski, C., Marco, S., 2006. Intraclast breccias in laminated sequences reviewed: recorders of paleo-earthquakes. *Geol. Soc. Spec. Pap.* 401, 195–214.
- Allen, C.D., Breshers, D.D., 1998. Drought-induced shift of a forest-woodland ecotone: rapid landscape response to climate variation. *Proc. Natl. Acad. Sci.* 95, 14839–14842.
- Andersen, K.K., Azuma, N., Barnola, J.M., Bigler, M., Biscaye, P., Cailion, N., Chappellaz, J., Clausen, H.B., Dahl-Jensen, D., Fischer, H., et al., 2004. High-resolution record of Northern Hemisphere climate extending into the last interglacial period. *Nature* 431, 147–151.
- Avni, Y., Porat, N., Plakht, J., Avni, G., 2006. Geomorphic changes leading to natural desertification versus anthropogenic land conservation in an arid environment, the Negev Highlands, Israel. *Geomorphology* 82, 177–200.
- Bar-Matthews, M., Ayalon, A., Gilmour, M., Matthews, A., Hawkesworth, C.J., 2003. Sea-level oxygen isotopic relationships from planktonic foraminifera and speleothems in the Eastern Mediterranean region and their implication for paleorainfall during interglacial intervals. *Geochim. Cosmochim. Acta* 67, 3181–3199.
- Bartov, Y., Stein, M., Enzel, Y., Agnon, A., Reches, Z., 2002. Lake levels and sequence stratigraphy of Lake Lisan, the Late Pleistocene Precursor of the Dead Sea. *Quat. Res.* 57, 9–21.
- Bartov, Y., Agnon, A., Enzel, Y., Stein, M., 2006. Late Quaternary faulting and subsidence in the central Dead Sea basin. *Isr. J. Earth Sci.* 55, 17–31.
- Bar-Yosef, O., 1991. Early Neolithic of the Levant: recent advances. *Rev. Archaeol.* 12, 1–18.
- Bar-Yosef, O., 1998a. On the nature of transitions: the Middle to Upper Palaeolithic and the Neolithic Revolution. *Camb. Archaeol. J.* 8, 141–163.
- Bar-Yosef, O., 1998b. The Natufian culture in the Levant, threshold to the origins of agriculture. *Evol. Anthropol.* 6, 159–177.
- Bar-Yosef, O., Gopher, A., 1997. An Early Neolithic Village in the Jordan Valley-Part I: The Archaeology of Netiv Hagdud. Harvard University, Cambridge, pp. 266.
- Ben-Avraham, Z., Garfunkel, Z., Lazar, M., 2008. Geology and evolution of the southern dead sea fault with emphasis on subsurface structure. *Annu. Rev. Earth Planet. Sci.* 36, 357–387.
- Breshers, D.D., Cobb, N.S., Rich, P.M., Price, K.P., Allen, C.D., Balice, R.G., Romme, W.H., Kastens, J.H., Floyd, M.L., Belnap, J., 2005. Regional vegetation die-off in response to global-change-type drought. *Proc. Natl. Acad. Sci.* 102, 15144–15148.
- Byrd, B.F., 1994. Public and private, domestic and corporate: the emergence of the southwest Asian village. *Am. Antiq.* 59, 639–666.
- Clift, P.D., 2006. Controls on the erosion of Cenozoic Asia and the flux of clastic sediment to the ocean. *Earth Planet. Sci. Lett.* 241, 571–580.
- Clift, P.D., Giosan, L., Blusztajn, J., Campbell, I.H., Allen, C., Pringle, M., Tabrez, A.R., Danish, M., Rabbani, M.M., Alizai, A., et al., 2008. Holocene erosion of the Lesser Himalaya triggered by intensified summer monsoon. *Geology* 36, 79.
- Dadson, S.J., Hovius, N., Chen, H., Dade, W.B., Hsieh, M.-L., Willett, S.D., Hu, J.-C., Horng, M.-J., Chen, M.-C., Stark, C.P., 2003. Links between erosion, runoff variability and seismicity in the Taiwan orogen. *Nature* 426, 648–651.
- Davis, S.J.M., 1991. When and why did prehistoric people domesticate animals? Some evidence from Israel and Cyprus. In: Bar-Yosef, O., Valla, F.R. (Eds.), *The Natufian culture in the Levant. International Monographs in Prehistory. Archaeological Series* 1, Ann Arbor, pp. 381–390.
- Edwards, P.C., House, E., 2007. The third season of investigations at the Pre-Pottery Neolithic A Site of Zahrat adh-Dhra' 2 on the Dead Sea Plain. *Jordan. Bull. Amer. Sch. Orient. Res.* 247, 1–19.
- Enzel, Y., Bookman, R., Sharon, D., Gvirtzman, H., Dayan, U., Ziv, B., Stein, M., 2003. Late Holocene climates of the Near East deduced from Dead Sea level variations and modern regional winter rainfall. *Quat. Res.* 60, 263–273.
- Foley, S.F., Gronenborn, D., Andreae, M.O., Kadereit, J.W., Esper, J., Scholz, D., Pöschl, U., Jacob, D.E., Schöne, B.R., Schreg, R., et al., 2013. The Palaeoanthropocene - the beginnings of anthropogenic environmental change. *Anthropocene* 3, 83–88.
- Goren, Y., Goring-Morris, A.N., 2008. Early pyrotechnology in the near east: experimental lime-plaster production at the Pre-Pottery Neolithic B site of Kfar HaHoresh, Israel. *Geochronology* 23, 779–798.
- Goring-Morris, A.N., Hovers, E., Belfer-Cohen, A., 2009. The dynamics of Pleistocene and Early Holocene settlement patterns and human adaptations in the Levant: an overview. In: Shea, J.J., Lieberman, D. (Eds.), *Transitions in Prehistory: Essays in Honor of Ofer Bar-Yosef*. Oxbow Books, Oxford, pp. 185–252.
- Grant, K.M., Rohling, E.J., Bar-Matthews, M., Ayalon, A., Medina-Elizalde, M., Ramsey,

- C.B., Satow, C., Roberts, A.P., 2012. Rapid coupling between ice volume and polar temperature over the past 150,000 years. *Nature* 491, 744–747.
- Haliva-Cohen, A., Stein, M., Goldstein, S.L., Sandler, A., Starinsky, A., 2012. Sources and transport routes of fine detritus material to the Late Quaternary Dead Sea basin. *Quat. Sci. Rev.* 50, 55–70.
- Hoffmann, T., Thorndycraft, V.R., Brown, A.G., Coulthard, T.J., Damnati, B., Kale, V.S., Middelkoop, H., Notebaert, B., Walling, D.E., 2010. Human impact on fluvial regimes and sediment flux during the Holocene: review and future research agenda. *Glob. Planet. Chang.* 72, 87–98.
- Hooke, R.L., 2000. On the history of humans as geomorphic agents. *Geology* 28, 843–846.
- Inbar, M., Tamir, M., Wittenberg, L., 1998. Runoff and erosion processes after a forest fire in Mount Carmel, a Mediterranean area. *Geomorphology* 24, 17–33.
- Istanbulluoğlu, E., 2005. Vegetation-modulated landscape evolution: effects of vegetation on landscape processes, drainage density, and topography. *J. Geophys. Res.* 110 (F02012).
- Kelly, A.E., Goulden, M.L., 2008. Rapid shifts in plant distribution with recent climate change. *Proc. Natl. Acad. Sci.* 105, 11823–11826.
- Ken-Tor, R., Agnon, A., Enzel, Y., Stein, M., Marco, S., Negendank, J.F.W., 2001. High-resolution geological record of historic earthquakes in the Dead Sea basin. *J. Geophys. Res.* 106 (B2), 2221–2234.
- Kenyon, K.M., 1957. *Digging Up Jericho*. Benn, London, pp. 272.
- Kuijt, I., Goring-Morris, N., 2002. Foraging, farming, and social complexity in the Pre-Pottery Neolithic of the southern Levant: a review and synthesis. *J. World Prehist.* 16, 361–440.
- Lague, D., Hovius, N., Davy, P., 2005. Discharge, discharge variability, and the bedrock channel profile. *J. Geophys. Res.* 110, F04006.
- Langgut, D., Neumann, F.H., Stein, M., Wagner, A., Kagan, E.J., Boaretto, E., Finkelstein, I., 2014. Dead Sea pollen record and history of human activity in the Judean Highlands (Israel) from the Intermediate Bronze into the Iron Ages (~2500–500 BCE). *Palynology* 38, 280–302.
- Lechevallier, M., 1978. *Abou Gosh et Beisamoun: deux gisements du VII millénaire avant l'ère chrétienne en Israël*. Association Paléorient, Paris, pp. 300.
- Litt, T., Ohlwein, C., Neumann, F.H., Hense, A., Stein, M., 2012. Holocene climate variability in the Levant from the Dead Sea pollen record. *Quat. Sci. Rev.* 49, 95–105.
- López-Merino, L., Leroy, S.A.G., Eshel, A., Epshtein, V., Belmaker, R., Bookman, R., 2016. Using palynology to re-assess the Dead Sea laminated sediments - indeed varves? *Quat. Sci. Rev.* 140, 49–66.
- Marc, O., Hovius, N., Meunier, P., Uchida, T., Hayashi, S., 2015. Transient changes of landslide rates after earthquakes. *Geology* 43, 883–886.
- Marco, S., Klinger, Y., 2014. Review of on-fault palaeoseismic studies along the Dead Sea Fault. In: Garfunkel, Z., Ben-Avraham, Z., Kagan, E. (Eds.), *Dead Sea Transform Fault System: Reviews*. Springer, Dordrecht, pp. 183–205.
- Marco, S., Stein, M., Agnon, A., Ron, H., 1996. Long-term earthquake clustering: a 50,000 years paleoseismic record in the Dead Sea Graben. *J. Geophys. Res.* 101, 6179–6192.
- McHugh, C.M., Kanamatsu, T., Seebur, L., Bopp, R., Cormier, M.-H., Usami, K., 2016. Remobilization of surficial slope sediment triggered by the AD 2011 Mw 9 Tohoku-Oki earthquake and tsunami along the Japan Trench. *Geology* 44, 391–394.
- Miebach, A., Chen, C., Litt, T., 2015. Last Glacial Vegetation and Climate Change in the Southern Levant. EGU General Assembly Conference Abstractspp. 3841.
- Migowski, C., 2001. *Untersuchungen laminierter holozäner Sedimente aus dem Toten Meer: Rekonstruktion von Paläoklima und-seismizität*. GeoForschungsZentrum Potsdampp. 99.
- Migowski, C., Agnon, A., Bookman, R., Negendank, J.F.W., Stein, M., 2004. Recurrence pattern of Holocene earthquakes along the Dead Sea transform revealed by varve-counting and radiocarbon dating of lacustrine sediments. *Earth Planet. Sci. Lett.* 222, 301–314.
- Molnar, P., 2001. Climate change, flooding in arid environments, and erosion rates. *Geology* 29, 1071–1074.
- Molnar, P., 2004. Late Cenozoic increase in accumulation rates of terrestrial sediment: how might climate change have affected erosion rates? *Annu. Rev. Earth Planet. Sci.* 32, 67–89.
- Molnar, P., Anderson, R.S., Kier, G., Rose, J., 2006. Relationships among probability distributions of stream discharges in floods, climate, bed load transport, and river incision. *J. Geophys. Res.* 111 (F02001).
- Molnar, P., Anderson, R.S., Anderson, S.P., 2007. Tectonics, fracturing of rock, and erosion. *J. Geophys. Res.* 112 (F03014).
- Montgomery, D.R., 2007. Soil erosion and agricultural sustainability. *Proc. Natl. Acad. Sci.* 104, 13268–13272.
- Montgomery, D.R., Schmidt, K.M., Greenberg, H.M., Dietrich, W.E., 2000. Forest clearing and regional landsliding. *Geology* 28, 311–314.
- Nadel, D., Nadler-Uziel, M., 2011. Is the PPNC really different? The flint assemblages from three layers at Tel Roim West, Hula Basin. In: Healey, E., Campbell, S., Maeda, O. (Eds.), *The State of the Stone Terminologies, Continuities and Contexts in Near Eastern Lithics*. Ex-orient, Berlin, pp. 243–256.
- Neugebauer, I., Brauer, A., Schwab, M.J., Waldmann, N.D., Enzel, Y., Kitagawa, H., Torfstein, A., Frank, U., Dulski, P., Agnon, A., et al., 2014. Lithology of the long sediment record recovered by the ICDP Dead Sea Deep Drilling Project (DSDDP). *Quat. Sci. Rev.* 102, 149–165.
- Neugebauer, I., Brauer, A., Schwab, M.J., Dulski, P., Frank, U., Hadzhiivanova, E., Kitagawa, H., Litt, T., Schiebel, V., Taha, N., et al., 2015. Evidences for centennial dry periods at ~3300 and ~2800 cal. yr BP from micro-facies analyses of the Dead Sea sediments. *The Holocene* 25, 1358–1371.
- Noy, T., 1989. Gilgal I: a Pre-Pottery Neolithic site, Israel - the 1985–1987 seasons. *Paléorient* 15, 11–18.
- Parker, R.N., Densmore, A.L., Rosser, N.J., de Michele, M., Li, Y., Huang, R., Whadcoat, S., Petley, D.N., 2011. Mass wasting triggered by the 2008 Wenchuan earthquake is greater than orogenic growth. *Nat. Geosci.* 4, 449–452.
- Perevolotsky, A., Seligman, N.G., 1998. Role of grazing in Mediterranean rangeland ecosystems. *Bioscience* 48, 1007–1017.
- Portenga, E.W., Rood, D.H., Bishop, P., Bierman, P.R., 2016. A late Holocene onset of aboriginal burning in southeastern Australia. *Geology* 44, 131–134.
- Prasad, S., Vos, H., Negendank, J.F.W., Waldmann, N., Goldstein, S.L., Stein, M., 2004. Evidence from Lake Lisan of solar influence on decadal- to centennial-scale climate variability during marine oxygen isotope stage 2. *Geology* 32, 581–584.
- Reusser, L., Bierman, P., Rood, D., 2015. Quantifying human impacts on rates of erosion and sediment transport at a landscape scale. *Geology* 43, 171–174.
- Rollefson, G.O., 1997. Changes in architecture and social organization at 'Ain Ghazal'. In: Rollefson, G.O., Gebel, H.G., Kafafi, Z.A.K. (Eds.), *Prehistory of Jordan II: Perspectives From 1997*. Ex oriente, Berlin, pp. 287–308.
- Rollefson, G.O., Köhler-Rollefson, I., 1989. The Collapse of Early Neolithic Settlements in the Southern Levant. In: Hershkovitz, I. (Ed.), *People and Culture in Change*. British Archaeological Reports, Oxford, pp. 73–89.
- Savage, S.H., Levy, T.E., 2016. *The Digital Archaeological Atlas of the Holy Land*.
- Singer, A., Ganor, E., Dultz, S., Fischer, W., 2003. Dust deposition over the Dead Sea. *J. Arid Environ.* 53, 41–59.
- Stein, M., 2001. The sedimentary and geochemical record of Neogene-Quaternary water bodies in the Dead Sea basin-inferences for the regional paleoclimatic history. *J. Paleolimnol.* 26, 271–282.
- Stein, M., Ben-Avraham, Z., Goldstein, S., Agnon, A., Ariztegui, D., Brauer, A., Haug, G., Ito, E., Yasuda, Y., 2011. Deep drilling at the Dead Sea. *Sci. Drill.* 46–47.
- Stiller, M., Gat, J.R., Kaushansky, P., 1997. Halite precipitation and sediment deposition as measured in sediment traps deployed in the Dead Sea: 1981–1983. In: Niemi, T.M., Ben-Avraham, Z., Gat, J. (Eds.), *The Dead Sea: The Lake and Its Setting*. Oxford Univ. press, USA, pp. 171–183.
- Syvitski, J.P., Vorosmarty, C.J., Kettner, A.J., Green, P., 2005. Impact of humans on the flux of terrestrial sediment to the global coastal ocean. *Science* 308, 376–380.
- Torfstein, A., Goldstein, S.L., Stein, M., Enzel, Y., 2013. Impacts of abrupt climate changes in the Levant from Last Glacial Dead Sea levels. *Quat. Sci. Rev.* 69, 1–7.
- Torfstein, A., Goldstein, S.L., Kushnir, Y., Enzel, Y., Haug, G., Stein, M., 2015. Dead Sea drawdown and monsoonal impacts in the Levant during the last interglacial. *Earth Planet. Sci. Lett.* 412, 235–244.
- Vanacker, V., von Blanckenburg, F., Govers, G., Molina, A., Poesen, J., Deckers, J., Kubik, P., 2007. Restoring dense vegetation can slow mountain erosion to near natural benchmark levels. *Geology* 35, 303–306.
- Waldmann, N., Torfstein, A., Stein, M., 2010. Northward intrusions of low-and mid-latitude storms across the Saharo-Arabian belt during past interglacials. *Geology* 38, 567–570.
- Wang, P., Scherler, D., Liu-Zeng, J., Mey, J., Avouac, J.P., Zhang, Y., Shi, D., 2014. Tectonic control of Yarlung Tsangpo Gorge revealed by a buried canyon in southern Tibet. *Science* 346, 978–981.
- Warren, S., 2001. Synopsis: Influence of Biological Soil Crusts on Arid Land Hydrology and Soil Stability. In: Belnap, J., Lange, O.L. (Eds.), *Biological Soil Crusts: Structure, Function, and Management*. Springer, Heidelberg, pp. 349–360.
- Whipple, K.X., 2001. Fluvial landscape response time: how plausible is steady-state denudation? *Am. J. Sci.* 301, 313–325.
- Wilkinson, B.H., 2005. Humans as geologic agents: a deep-time perspective. *Geology* 33, 161–164.
- Wilkinson, B.H., McElroy, B.J., 2007. The impact of humans on continental erosion and sedimentation. *Geol. Soc. Am. Bull.* 119, 140–156.
- Zeder, M.A., 2011. The origins of agriculture in the near east. *Curr. Anthropol.* 52, S221–S235.
- Zhang, P.Z., Molnar, P., Downs, W.R., 2001. Increased sedimentation rates and grain sizes 2–4 Myr ago due to the influence of climate change on erosion rates. *Nature* 410, 891–897.
- Zheng, H., Powell, C.M., An, Z., Zhou, J., Dong, G., 2000. Pliocene uplift of the northern Tibetan plateau. *Geology* 28, 715–718.